Journal of African Earth Sciences 60 (2011) 328–336

Contents lists available at ScienceDirect

Journal of African Earth Sciences

journal homepage: www.elsevier.com/locate/jafrearsci

Upper mantle structure of the Saharan Metacraton

Mohamed G. Abdelsalam [a,*], Stephen S. Gao [a], Jean-Paul Liégeois [b]

[a] Missouri University of Science and Technology, Department of Geological Sciences and Engineering, 1400 N, Bishop, Rolla, MO 65401, United States
[b] Royal Museum for Central Africa, Section of Isotope Geology, B-3080 Tervuren, Belgium

ARTICLE INFO

Article history:
Received 3 August 2010
Received in revised form 17 March 2011
Accepted 28 March 2011
Available online 7 April 2011

Keywords:
Saharan Metacraton
Upper mantle structure
Delamination
Convective removal
Metacratonization

ABSTRACT

The ~500,000 km^2 Saharan Metacraton in northern Africa (metacraton refers to a craton that has been mobilized during an orogenic event but that is still recognisable through its rheological, geochronological and isotopic characteristics) is an Archean–Paleoproterozoic cratonic lithosphere that has been destabilized during the Neoproterozoic. It extends from the Arabian–Nubian Shield in the east to the Trans-Saharan Belt in the west, and from the Oubanguides Orogenic Belt in the south to the Phanerozoic cover of North Africa. Here, we show that there are high S-wave velocity anomalies in the upper 100 km of the mantle beneath the metacraton typical of cratonic lithosphere, but that the S-wave velocity anomalies in the 175–250 km depth are much lower than those typical of other cratons. Cratons have possitive S-wave velocity anomalies throughout the uppermost 250 km reflecting the presence of well-developed cratonic root. The anomalous upper mantle structure of the Saharan Metacraton might be due to partial loss of its cratonic root. Possible causes of such modification include mantle delamination or convective removal of the cratonic root during the Neoproterozoic due to collision-related deformation. Partial loss of the cratonic root resulted in regional destabilization, most notably in the form of emplacement of high-K calc-alkaline granitoids. We hope that this work will stimulate future multi-national research to better understand this part of the African Precambrian. Specifically, we call for efforts to conduct systematic geochronological, geochemical, and isotopic sampling, deploy a reasonably-dense seismic broadband seismic network, and conduct systematic mantle xenoliths studies.

1. Introduction

Africa's Precambrian crust is largely dominated by either Archean–Paleoproterozoic cratons or Neoproterozoic orogenic belts (Fig. 1; Meert and Lieberman, 2007). However, the ~500,000 km^2 tract of continental lithosphere bounded by the Arabian–Nubian Shield in the east, the Trans-Saharan Orogen in the west, and the Congo Craton in the south (Fig. 1) cannot be considered as a craton or an orogenic belt because of conflicting geological, geochronological and isotopic observations. Nevertheless, many workers have treated this region as a craton giving it the name Nile Craton (Rocci, 1965), Sahara-Congo Craton (Kröner, 1977), Eastern Saharan Craton (Bertrand and Caby, 1978), or Central Saharan Ghost Craton (Black and Liégeois, 1993), a name that reflects the peculiar characteristics of this Precambrian block. Abdelsalam et al. (2002) have proposed the name "Saharan Metacraton" for this region where they defined a "metacraton" as a "craton that has been variably mobilized during an orogenic event but that is still recognisable through its rheological, geochronological and isotopic characteristics". Neoproterozoic destabilization of the region occupied by the Saharan Metacraton was first recognized by Kennedy (1964) who introduced the term "Pan-African tectono-thermal event". However, Kennedy (1964) considered this region as indistinguishable from other Neoproterozoic orogenic belts in Africa. In their synthesis, Abdelsalam et al. (2002) agreed that the Saharan Metacraton has been destabilized at the end of the Neoproterozoic era, but the metacraton has acted as a coherent rheological entity, hence cannot simply be considered as an orogenic belt with remnants of older reworked components.

Seismic tomography studies of global scale (Grand, 2002; Shapiro and Ritzwoller, 2002; Lebedev et al., 2009; Pasyanos, 2010), Africa-wide (Ritsema and van Heijst, 2000; King and Ritsema, 2000; Deen et al., 2006; Pasyanos and Nyblade, 2007; Begg et al., 2009), and those focused on parts of Africa (James et al., 2001; Priestley et al., 2006) have been successful in imaging the West African, Congo, and Kalahari Cratons as blocks with well-developed cratonic roots that extend down to a depth of 250 km. However, these studies, with the exception of Deen et al. (2006), Begg et al. (2009), and Pasyanos (2010) did not directly address the state of the sub-continental lithospheric mantle (SCLM) beneath the Saharan Metacraton. Here, we use the term SCLM to refer to the chemically depleted rigid lower part of the continental plate

* Corresponding author. Tel.: +1 573 341 4100; fax: +1 573 341 6935.
E-mail addresses: abdelsam@mst.edu (M.G. Abdelsalam), sgao@mst.edu (S.S. Gao), jean-paul.liegeois@africamuseum.be (J.-P. Liégeois).

1464-343X/$ - see front matter © 2011 Elsevier Ltd. All rights reserved.
doi:10.1016/j.jafrearsci.2011.03.009

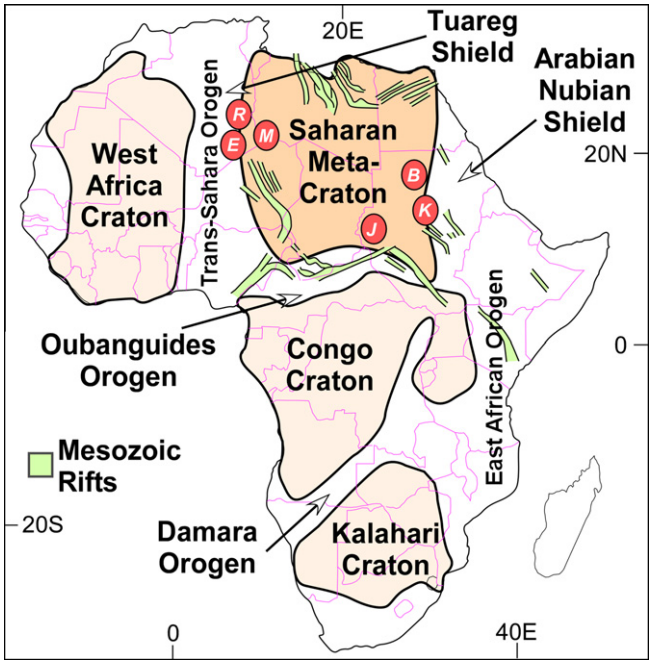

Fig. 1. Africas' Precambrian cratons, metacratons and orogenic belts (modified after Meert and Lieberman, 2007). B = Bayuda; J = Jebel Mara; R = Raghane Shear Zone; K = Keraf-Kabus–Sekerr Suture; U = Uweinat; M = Murzuq Craton; E = Eastern Hoggar.

that moves with the plate which is isolated from the convective mantle (hence resists homogenization), and the base of it coincides with the low velocity zone (O'Reilly et al., 2001).

In this work we present new insights of the Saharan Metacraton SCLM by reprocessing the S-wave velocity model of Grand (2002) and compare the Saharan Metacraton with other African cratons. Subsequently, we discuss the metacraton's evolution by considering models involving Neoproterozoic mantle delamination, thermal erosion through convective removal of the cratonic root, or upper mantle structural modification through thermal activities associated with Phanerozoic events in northern Africa. Finally, we present recommendations for future research aimed at better understanding the geodynamic evolution of the Saharan Metacraton throughout the geological time.

2. Tectonic setting of the Saharan Metacraton

The geology and geochronology of the Saharan Metacraton are outlined in Abdelsalam et al. (2002). The region is dominated by gneisses and migmatites outcrops with few places where the metamorphic grade reaches granulite facies. In some places, low-grade greenschist facies metamorphic rocks of Neoproterozoic age crop out within the Saharan Metacraton. The metacraton is bounded in the east, west, and south by lithospheric-scale suture zones resulting from Neoproterozoic collision events with the surrounding terranes. To the east, the N-trending Keraf–Kabus–Sekerr Shear Zone (Fig. 1) is interpreted as an arc-continental suture separating the Saharan Metacraton from the Arabian–Nubian Shield which represents the northern part of the East African Orogen (Abdelsalam and Dawoud, 1991; Stern, 1994; Abdelsalam et al., 1996). An old continental crust has been demonstrated to be located in the Bayuda Desert in northern Sudan just east of the Keraf–Kabus–Sekerr shear zone (Fig. 1; Küster et al., 2008). Similarly, the N-trending Raghane Shear Zone to the west (Fig. 1) is interpreted as a suture defining the collision zone between the metacraton and the Tuareg Shield which represents the northern part of the Trans-Saharan Orogen (Liégeois et al., 1994, 2003; Henry et al., 2009). To the south, the Saharan Metacraton is separated from the Congo Craton by the E-trending Oubanguides Orogen (Fig. 1) which is interpreted as imbricated Neoproterozoic and Archean–Paleoproterozoic thrust sheets tectonically emplaced southward onto the Congo Craton (Pin and Poidevin, 1987; Toteu et al., 2006).

Geochronological and isotopic data from the Saharan Metacraton are highly variable as exemplified by the wide range of ages (500–3100 Ma), especially Nd model ages (Abdelsalam et al., 2002; Shang et al., 2010). Archean–Paleoproterozoic ages within the metacraton using Rb–Sr and U–Pb zircon systematics have been reported for gneissic and granulitic rocks by Klerkx and Deutsch (1977), Pin and Poidevin (1987), Sultan et al. (1994), and Stern et al. (1994). However, widespread late Neoproterozoic igneous activity in the form of high-K calc-alkaline granitoids is present within the Saharan Metacraton as evident from Rb–Sr and U–Pb crystallization ages that overwhelmingly clustered between 650 and 550 Ma (Ashwal and Burke, 1989; Black and Liégeois, 1993; Shang et al., 2010; Fezaa et al., 2010).

3. Seismological data

We used the Grand (2002) model to generate S-wave velocity anomaly images and cross sections at various depths of the Saharan Metacraton lithospheric column (Figs. 2 and 3). We discuss results of the seismic tomography by focusing on the 0–100 km, 100–175 km, and 175–250 km depths. Subsequently, we present results from a difference S-wave velocity image in which velocity anomalies at 175–250 km depth are subtracted from those at 0–100 km depth. Additionally, we compare the S-wave depth variation of the Saharan Metacraton with those of tectonically-active and stable continental regions. It should be mentioned here that there are only a few broad-band seismic stations within and around the Saharan Metacraton and results of this study are based on data acquired from seismic broadband stations deployed around the World (see Fig. 2 of Grand (2002)). Regardless, Grand (2002) model made advantage of multi-bounce shear phases for covering regions with limited number of seismic broadband stations such as the Saharan Metacraton (see Fig. 3 of Grand (2002)). These multi-bounce shear phases which include SS, SSS, and SSSS improve the resolution of the seismic data compared to the level that would have been achieved through the reliance of acquiring S-wave velocity data from only the seismic broadband stations over the Saharan Metacraton. Additionally, Begg et al. (2009) concluded (from comprehensive examination of the resolution of Grand (2002) model including checkerboard test) that the overall resolution of the data is adequate for imaging the S-wave velocity structure of the upper mantle under Africa. Further, the close similarities between previous seismic tomography results using different seismic phases and/or tomographic imaging techniques with results discussed below suggest that major features of the upper mantle beneath the Saharan Metacraton are well-resolved.

3.1. 0–100 km Depth

At 0–100 km depth (Figs. 2A and 3) the West Africa, Congo, and Kalahari Cratons are characterized by significantly faster S-wave velocity anomalies compared to other regions in Africa. In these regions the S-wave velocities are up to 6% faster relative to the Preliminary Reference Earth Model (PREM) (Dziewonski and Anderson, 1981). Similarly, the Saharan Metacraton is marked by faster S-wave velocities comparable to those of the West Africa, Congo and Kalahari Cratons. The southern and western boundaries of the metacraton are particularly distinct where the Trans-Saharan and the Oubanguides Orogen are marked by belts of lower

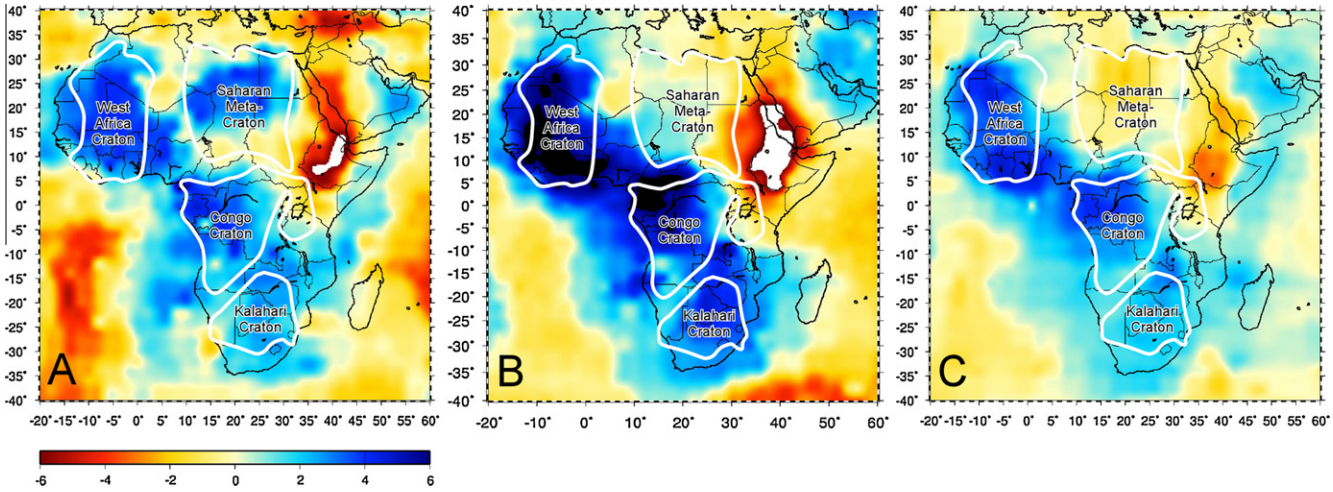

Fig. 2. Shear wave velocity anomalies underneath Africa at: (A) 0–100 km; (B) 100–175 km. (C) 175–250 km. Color bar indicates percentage difference of S-wave velocity relative to the Preliminary Reference Earth Model (PREM); Data from Grand (2002) model.

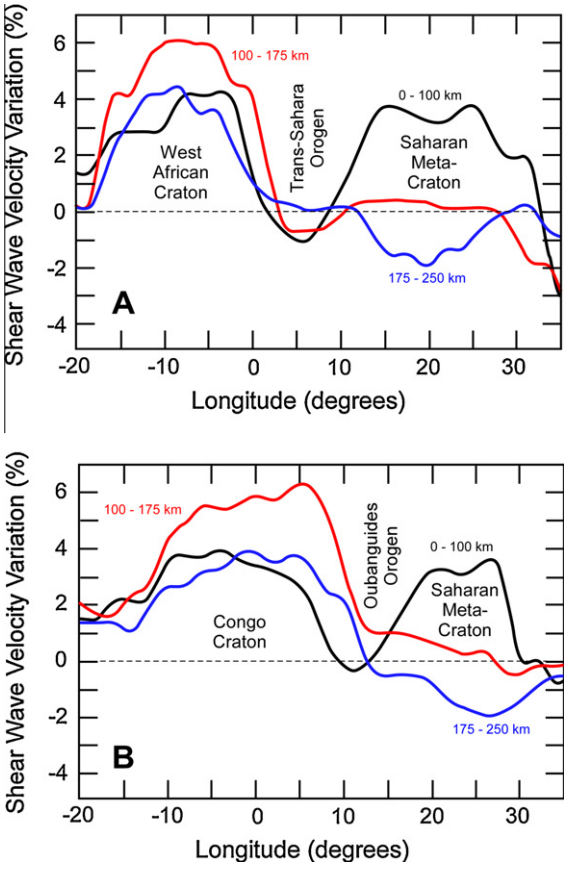

Fig. 3. (A) E–W sections across Africa along latitude 25°N showing S-wave velocity anomalies at 0–100 km; 100 and 175 km; and 175–250 km. (B) N–S sections across Africa along longitude 20°E showing S-wave velocity variation at 0–100 km; 100–175 km; and 175–250 km. Data from Grand (2002) model.

S-wave velocity anomalies. This is particularly evident from the E–W and N–S cross-sections following latitude 25°N and longitude 20°E, respectively (Figs. 3A and B). The S-wave velocity variation across the West Africa Craton and the Saharan Metacraton peaks to 4% increase relative to PREM in the central parts of these blocks. However, the S-wave velocity anomalies drop sharply as the Trans-Saharan Orogen is approached from east and west to reach −1% relative to PREM in the central part of the orogen. Similarly, the Congo Craton and the Saharan Metacraton show S-wave velocities that are 4% higher than PREM in their central parts. However, the S-wave velocities decrease to reach those of PREM over the Oubanguides Orogen. It is not clear whether the slower S-wave velocity structures underlying the Oubanguides Orogen reflect the deeper manifestation of the Precambrian structure or those are associated with Mesozoic rift structures (Fig. 1). Rift structures are generally characterized by slower S-wave velocities relative to PREM at 80–150 km depth because of asthenospheric upwelling (e.g. Dugda et al., 2009). Many of these rift structures in northern and eastern Africa closely coincide with, and follow the southern and eastern margins of the Saharan Metacraton (Fig. 1). It is worth mentioning here that recent broad-band seismic surface-wave dispersion analysis found that shear wave velocity is considerably higher under cratons compared to Proterozoic orogenic belts (Lebedev et al., 2009). This velocity difference is attributed to a colder SCLM under cratons compared to orogenic belts rather than compositional difference (Lebedev et al., 2009).

The observed faster S-wave velocity anomalies at 0–100 km depth beneath the West African, Congo, and Kalahari Cratons are in good agreement with results from other tomography imaging of the SCLM beneath Africa, especially those of Ritsema and van Heijst (2000), Shapiro and Ritzwoller (2002), Pasyanos and Nyblade (2007), Lebedev et al. (2009), and Begg et al. (2009). In all these tomographic models, the SCLM of these cratons is shown to have seismic wave velocities as much as 6% faster than PREM. However, with the exception of Begg et al. (2009), these models did not discuss the Saharan Metacraton as a separate entity at the 0–100 lithospheric level. Nevertheless, in their imaging of the African SCLM, Ritsema and van Heijst (2000) used fundamental-mode Rayleigh wave phase velocity analysis to report at 0–100 km depth "a relatively high S-wave velocity beneath Egypt" that coincides with parts of what is subsequently referred to as the Saharan Metacraton by Abdelsalam et al. (2002). Pasyanos and Nyblade (2007) used group velocity measurements of fundamental-mode Rayleigh and Love wave velocities to image the crust and SCLM beneath Africa. Although it has not been discussed, the 0–100 km S-wave velocity slice of Pasyanos and Nyblade (2007) shows much of Egypt and eastern Libya underlain by an S-wave velocity anomaly that is ~6% faster than PREM. Lebedev et al. (2009) used a combination of waveform-analysis and measured inter-station Rayleigh and Love-wave phase velocities to develop a global tomographic model. At 110 km depth, this model shows a

tongue of ~4% faster velocity relative to PREM that extends from the eastern Mediterranean throughout western Egypt and down to northwestern Sudan. Additionally, Begg et al. (2009), using S-wave tomography derived from shear body-wave travel times based on the Grand (2002) model, imaged the Saharan Metacraton as a separate entity defined by "visible knobs" with velocities that are ~4% faster relative to PREM.

3.2. 100–175 km Depth

At 100–175 km depth the West African, the Congo, and the Kalahari Cratons show velocities that are up to 6% faster than PREM (Figs. 2B and 3) similar to those of Ritsema and van Heijst (2000), Shapiro and Ritzwoller (2002), Deen et al. (2006), Pasyanos and Nyblade (2007), and Begg et al. (2009) models. However, the faster S-wave velocity anomalies observed at 0–100 km depth under the Saharan Metacraton decrease sharply to nearly zero at 100–175 km depth (Fig. 3). The Ritsema and van Heijst (2000) model shows that the faster S-wave velocity under Egypt persists down to a depth of 150 km, but this disappears at 200 km depth where much of the Saharan Metacraton is shown as been underlain by velocities equal to PREM. Additionally, the Saharan Metacraton was imaged as underlain by a slightly higher velocity relative to PREM at 100–175 km in Deen et al. (2006) using S-wave velocity model derived from Grand (2002). The velocity values were not specified in the presentation of Deen et al. (2006), but it can be concluded that these are not as high as those under other African cratons. On the other hand, at 150 km depth, the Pasyanos and Nyblade (2007) model shows the Saharan Metacraton as being spotted with velocities as 6% faster and −6% slower than PREM. However, at 200 km depth, the Pasyanos and Nyblade (2007) model shows the metacraton as being underlain by uniform velocities equaling PREM with the exception of southwestern Egypt and northwestern Sudan where faster S-wave velocities are observed. Begg et al. (2009) model at 100–175 km depth shows the Saharan Metacraton as an incoherent region spotted with velocities that are slightly (~2%) higher than PREM. Pasyanos (2010) used long-period S-wave dispersion analysis to image global lithospheric thickness and concluded that there is a clear boundary between the Saharan Metacraton on one hand and the West African Craton in the west and the Congo craton in the south on the other hand. Additionally, Pasyanos (2010) noted that the lithospheric thickness results clearly indicate that the Saharan Metacraton lithosphere was disrupted perhaps due to Neoproterozoic remobilization as suggested by Abdelsalam et al. (2002). Such a disruption has also been recently described in the western part of the Saharan Metacraton close to Eastern Hoggar (Fig. 1; Fezaa et al., 2010).

3.3. 175–250 km Depth

The S-wave velocities under the Saharan Metacraton at 175–250 km depth are ~2% slower than PREM which are sharply different from those beneath other African cratons (Figs. 2C and 3). These S-wave velocity anomalies are similar to those observed by Ritsema and van Heijst (2000), Shapiro and Ritzwoller (2002), Pasyanos and Nyblade (2007), and Begg et al. (2009).

3.4. 0–100 km–175–250 Differential velocities and S-wave velocity depth variation

To evaluate S-wave velocity distribution as a function of depth under Africa and worldwide, we have generated S-wave differential velocity images by subtracting the S-wave velocity anomalies at 175–250 km depth from those at 0–100 km depth (Fig. 4). Regions that are underlain by stable cratons with well-developed lithospheric roots are expected to show very low S-wave velocity differences, because the S-wave velocity anomalies would be approximately uniform throughout the 250 km column of SCLM. This is certainly the case of the Congo, the Kalahari, and the West African Cratons (Fig. 4B). On the other hand, regions that are underlain by young orogenic belts and recently rifted continental margins are expected to be defined by negative S-wave differential velocities as in the case of Afar (Fig. 4B). However, the S-wave velocity difference under the Saharan Metacraton is strikingly higher than those expected for typical cratons (Fig. 4B). Globally, no continental area of this size has a comparable velocity contrast between the shallow SCLM and the 175–250 km depth range (Fig. 4A). These images also define the Saharan Metacraton as a distinctive entity with boundaries approximating those inferred from surface geology (Fig. 4B). This can be explained by that the cratonic root under the Saharan Metacraton has been partially removed allowing the asthenosphere to ascend closer to the lower crust.

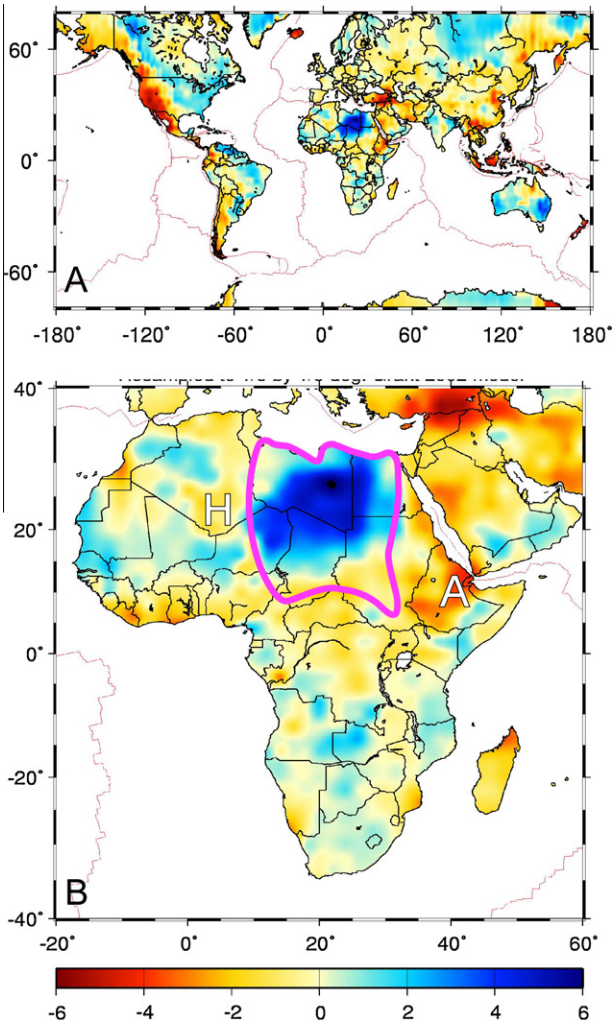

Fig. 4. Differential S-wave velocity images of: (A) the World; and (B) Africa generated by subtracting the S-wave velocities at 175–250 km depth from those at 0 to 100 depth. A = Afar. H = Hoggar Swell. Heavy pink line represents the boundary of the Saharan Metacraton as defined by surface geology. Color bar indicates the difference between the 0–100 and 175–250 km depth percentage difference in S-wave velocity relative to Preliminary Reference Earth Model (PREM). Data from Grant (2002) model. (For interpretation of the references to color in this figure legend, the reader is referred to the web version of this article.)

The above results are re-enforced by evaluating the depth variations of the S-wave velocities under the Saharan Metacraton (Fig. 5). At shallower depth (~50 km) the S-wave velocity under the metacraton is similar to that of stable continental regions as estimated by Grand and Helmberger (1984). However, as the depth

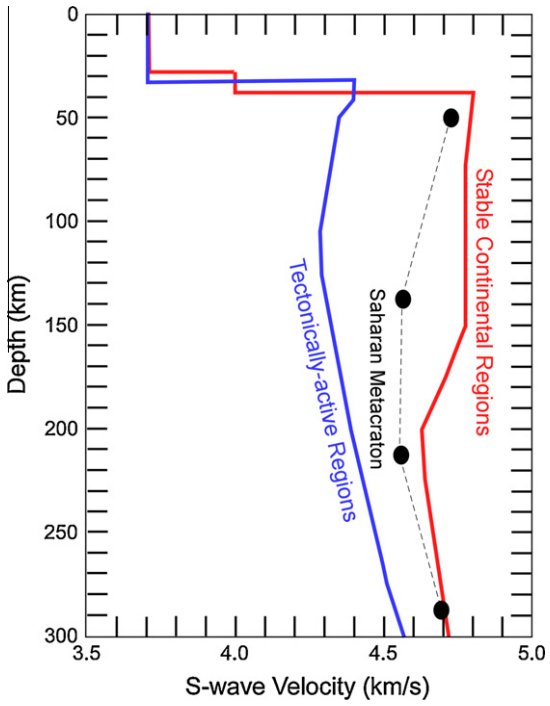

Fig. 5. Depth variation of S-wave velocities of the Saharan Metacraton compared to those of stable continental regions and tectonically-active regions. S-wave velocities of stable continental regions and tectonically-active regions are from Grand and Helmberger (1984).

increases (especially between ~100 and ~200 km) the S-wave velocities under the Saharan Metacraton become slower than those of stable continental regions and moves towards those which are typical of tectonically-active regions (Fig. 5).

4. Thickness and age of the cratonic root under the Saharan Metacraton

Our analysis suggests that the SCLM beneath the Saharan Metacraton continues to a depth of at least 100 km. However, it is not certain how much deeper beyond 100 km this root extends. This is particularly complicated by the diffused nature of the lithosphere–asthenosphere boundary (Eaton et al., 2009). Eaton et al. (2009) suggested that under cratons this boundary is defined by a dislocation creep deformation zone that is ~20 km thick in presence of fluids, but this can be ~50 km thick in dry conditions. Regardless, it is certain that the root beneath the Saharan Metacraton is thinner than those of other African cratons as our results show as well as results from other researchers, especially Pasyanos (2010). Also, in addition to seismic tomography results discussed above, global thermal modeling of mantle temperature (Artemieva, 2006, 2009) suggests that much of the Saharan Metacraton is underlain by ~150 km thick SCLM. Artemieva (2009) also re-evaluated Grand (2002) and Shapiro and Ritzwoller (2002) seismic tomography models to present images in which the Saharan Metacraton SCLM is shown to have a depth of 100–150 km.

The SCLM of the Saharan Metacraton is probably pre-Neoproterozoic in age, but it has been affected by thermal and deformation events during the Neoproterozoic Pan-African and younger Cenozoic events. Neoproterozoic disturbance of the pre-Neoproterozoic lithosphere of the Saharan Metacraton has been recently documented by Fezaa et al. (2010) from Eastern Hoggar which is located along the western margin of the Saharan Metacraton (Fig. 1). Fezaa et al. (2010) concluded that this region had acted as a craton until ~570 Ma. This conclusion is based on detrital zircon results which showed that the region was covered between 590 and 570 by a sedimentary sequence in which the source of these detrital zircons was the Tuareg Shield to the west of Eastern Hoggar (Fig. 1). Fezaa et al. (2010) have shown that Eastern Hoggar was subsequently dissected at 570–550 Ma by NW-trending shear zones broadly defining the western boundary of the Murzug Craton (Fezaa et al., 2010) which represents part of the western extension of the Saharan Metacraton (Fig. 1). These shear zones were reactivated during the Mesozoic by a NW-trending rift system (Fig. 1). Further, Fezaa et al. (2010) suggested that these shear zones were developed in an intra-continental tectonic setting and they were associated with metacratonization processes. Fezaa et al. (2010) finalized that the Murzuk craton was not affected by such metacratonization processes and retained its cratonic behavior throughout its geological history as evidenced by its seismic tomography structure which reflects high S-wave velocity in Pasyanos and Nyblade (2007) model.

Nd model ages from mantle xenoliths from Jebel Mara in western Sudan (Fig. 1) gave ages of 2820, 2210, 1930, and 790 Ma (Davidson and Wilson, 1989). Lucassen et al. (2008) concluded from isotopic studies of mantle xenoliths from the Bayuda Desert in northern Sudan (Fig. 1) that the SCLM of the Saharan Metacraton is an old depleted mantle which was formed and separated from the convective mantle before the Neoproterozoic Pan-African event ~1 Ga ago. This conclusion was based on the presence of non-radiogenic Pb and Sr in some of the samples. However, Lucassen et al. (2008) also concluded, on the basis of Sr, Nd, and Pb isotopic ratios, that the SCLM of the Saharan Metacraton must have been heavily metasomatized during the Neoproterozoic time. Additionally, Lucassen et al. (2008) noted that the depleted trace elements patterns observed in some of the mantle xenoliths suggested a Cenozoic melt extraction from the upper part of the SCLM of the Saharan Metacraton. Deen et al. (2006) and Begg et al. (2009) concluded from geotherm and density calculations that the Saharan Metacraton SCLM is dominantly Proterozoic in age with more fertile composition compared to other African cratons with the exception of small regions such as Uweinat (Fig. 1) that might be underlain by less fertile Archean SCLM.

5. Discussion

5.1. Decratonization and metacratonization

Cratons are underlain by thick, cold, anhydrous and strong SCLM dominantly composed of forsterite-rich olivine and orthopyroxene. Such physical and chemical characteristics make this mantle lithosphere buoyant and barren, isolating it from convicting mantle, allowing for a long-lasting stability and paucity of significant magmatism and tectonism (Pollack, 1986; Hirth et al., 2000; Yang et al., 2008; Arndt et al., 2009). However, this stability may not be permanent and cratons can lose their stable SCLM. This results in "decratonization" where lithospheric strength is lost, even though isotopic characteristics of the crust are likely to survive (Yang et al., 2008). However, as in the case of the Saharan Metacraton, these destabilization processes might not result in a complete loss of cratonic characteristics. Hence, we prefer to use the term "metacratonization" for such cases.

5.2. Other examples of cratonic remobilization

Besides the Saharan Metacraton, the North China Craton in China (Kusky et al., 2007a,b; Zhai et al., 2007) and the Wyoming Craton (Keller, 2008; Foster et al., 2008) in the US might represent other examples of cratonic remobilization. Seismic tomography models of the North China Craton indicate significant thinning of

the lithosphere and cratonic root loss under the eastern part of the craton (e.g. Huang and Zhao, 2004; Zhao et al., 2009; Tin et al., 2009; An et al., 2009; Santosh et al., 2010). These models have shown that the lithosphere in the eastern part of the North China Craton is only ~100 km thick compared to the ~250 km thickness in the western part. It is generally agreed that the cratonic root loss occurred between 140 and 120 Ma as indicated by the timing of basins formation, deformation, and change in type of magmatism and mantle xenolithes sampled by magmatism and kimberlite pipes (Kusky et al., 2007a). However, different hypotheses are offered to explain the processes through which the cratonic root was lost. Kusky et al. (2007a) summarized these into four broad models including mechanical disruption of the SCLM through collisional and rifting events; incremental thermo-chemical erosion of the SCLM accompanying asthenospheric upwelling of a mantle wedge (convective removal); mantle lithosphere delamination or density foundering resulting in sinking of the thickened SCLM into the convective mantle; or hydro-weakening of the SCLM through repeated subduction events.

The proposition that the cratonic root of the Wyoming Craton was lost was suggested by van der Lee and Nolet (1997). Subsequently, Foster et al. (2008) and Keller (2008) proposed that the SCLM of the craton is delaminating from west to east, mostly due to the Yellowstone hot spot. Additionally, Keller (2008) eluded to that, in addition to the hot spot, the Wyoming craton has been decratonized since ~100 Ma due to tectonic activities in the western margin of the North American plate. These interpretations are in good agreement with a recent seismic tomography model acquired through the deployment of seismic broadband stations of the USArray (Burdick et al., 2010). In this model the eastern part of the Wyoming Craton is imaged as possessing a cratonic root to a depth of ~300 km. However, the western part of the craton shows a NE-trending encroachment of a low *P*-wave velocity band (typical of asthenospheric material) that coincides with the Snake River Plain.

5.3. Consequences of cratonic remobilization

Cratonic remobilization is manifested by widespread destabilization including uplift, igneous activities, high-temperature metamorphism, and extension. This destabilization is thought to be associated with SCLM thinning after its thickening through shortening which usually accompanies collision and convergence, and/or metasomatism (Kay and Kay, 1993; Begg et al., 2009; Arndt et al., 2009). Thickening of the SCLM will further be facilitated by additional negative buoyancy force when denser cratonic roots are formed (Schott and Schmeling, 1998). However, we argue here that this might not be the evolutionary pass leading to metacratonization as exemplified by the Saharan Metacraton. It is apparent from its western part that the Saharan Metacraton had partially preserved its old cratonic characteristics when it was destabilized as evidenced by the presence of meta-volcanic rocks (De Waele et al., 2006), over-thrust ophiolitic complexes (Ennih and Liégeois, 2008), and granulite facies metamorphic assemblages (Bendaoud et al., 2008). The presence of these rocks, which are older than the main Pan-African orogenic phase, suggests the existence of a rigid craton at that time.

5.4. Possible mechanisms for metacratonization

Theoretically, thinning of the SCLM can occur through sub-lithospheric mantle delamination (Bird, 1979; Avigad and Gvirtzman, 2009), convective removal (England, 1993), or simply heating, especially by an uprising mantle plume (Ebinger and Sleep, 1998). In this section, we examine possible explanations for the unusual SCLM of the Saharan Metacraton by considering mechanisms involving mantle delamination or convective removal of the Saharan Metacraton root during the Neoproterozoic. Additionally, we argue that Phanerozoic heating of the Saharan Metacraton SCLM was not the most important cause of thinning. This is in accordance with Liégeois et al. (2005) conclusion who considered removal of the Saharan Metacraton's SCLM through thermal conduction associated with a rising mantle plume is highly unlikely. This discussion has to be taken with the understanding that it is possible that more than one mechanism might have contributed to the modification of the metacraton's SCLM and that future research involving higher resolution seismic tomography and mantle xenoliths geochemistry is desired to resolve the conundrum of the Saharan Metacraton.

5.4.1. Mantle lithosphere delamination

Delamination generally occurs through the complete detachment and sinking of the SCLM and the lower crust allowing for the asthenosphere to be at direct contact with the crust resulting in rapid uplift and extension (Kay and Kay, 1993). To explain Neoproterozoic destabilization of the region underlain by the Saharan Metacraton, Ashwal and Burke (1989) suggested that the SCLM beneath North Africa was separated from the crust after thickening as a result of Neoproterozoic collision. Similarly, Black and Liégeois (1993) proposed that Neoproterozoic delamination affected most of a once Saharan craton and that the region around Uweinat (Fig. 1) is the only undisturbed cratonic fragment. Recently, Fezaa et al. (2010) argued that the Murzuk Craton (Fig. 1) also survived metacratonization. Further, Black and Liégeois (1993) concluded that delamination at the end of the Neoproterozoic that juxtaposed the crust against hot asthenosphere can explain many of the Pan-African tectono-thermal activities in the region including reactivation of old terrane boundaries, abundant late-tectonic high-K calc-alkaline granitoids, high-temperature low-pressure metamorphism, displacement along regional-scale shear zones, and emplacement of mantle-derived post-tectonic granitoids. Recently, Shang et al. (2010) concluded that migmatization and granitization within the Saharan Metacraton which occurred at ~600 Ma are closely related in space and time. Further, Shang et al. (2010) argued that migmatization and granitization of the metacraton might have been related to high heat flow resulting from Neoproterozoic crust-mantle delamination. Alternatively, Liégeois et al. (2003) and Fezaa et al. (2010) proposed that delamination along major shear zones can be an effective process for metacratonization. Liégeois et al. (2003) argued that the spatial resolution of the current seismic tomography data over North Africa is not high enough to distinguish between partially and completely delaminated regions.

The observed upper mantle structure below the Saharan Metacraton suggests that its upper 100 km SCLM is similar to that of other cratons. This lithospheric structure indicates that the Saharan Metacraton has thickened an unknown amount due to Phaneozoic cooling. Avigad and Gvirtzman (2009) proposed that the northern part of the Arabian–Nubian Shield might have suffered rapid lithospheric mantle delamination at ~630 Ma resulting in a complete removal of the mantle lithosphere. They used numerical modeling results to show that it might have taken ~100 Ma after delamination for the mantle lithosphere under the northern part of the Arabian–Nubian Shield to grow to a thickness of ~100 km.

Here (accounting for the possibility of absence of growth of the mantle lithosphere under the Saharan Metacraton subsequent to delamination) we propose an alternative model that involves a less dramatic delamination at the Mechanical Boundary Layer (MBL) – Thermal Boundary Layer (TBL) interface as a possible explanation for the upper mantle structure of the Saharan Metacraton. Typical upper mantle below cratons generally comprises a cold and rigid upper layer with a brittle behavior (MBL) and a warmer and ductile lower layer (TBL). Multi-mode surface wave data and geotherm

studies from southern Africa (Priestley et al., 2006) indicate that the MBL under cratonic regions is 175 ± 25 km whereas the thickness of the TBL is ~200 km. The TBL passes progressively into the asthenosphere, its base is considered to be transient, and its thermal characteristics are indistinguishable from those of the asthenosphere. Removal of the TBL and subsequent implication of cratonic remobilization have been previously proposed for other regions such as the Tibetan Plateau (England, 1993).

The Saharan Metacraton collided during the Neoproterozoic with the Arabian–Nubian Shield in the east, the Trans-Sahara Orogen in the west, and the Oubanguides orogen in the south. The metacraton might have also collided with an unknown continental block in the north and the manifestation of this collision is referred to by Fezaa et al. (2010) as the Murzukian episode. These collision events might have resulted in reactivation of pre-existing zones of lithospheric weaknesses leading in some places to overgrowth of the cratonic root allowing for negative buoyancy to develop. The negative buoyancy might have been re-enforced by metasomaism during the Neoproterozic time (Lucassen et al., 2008) by making the cratonic root more hydrous and denser. Subsequently, delamination at the MBL-TBL occurred resulting in a widespread remobilization of the Saharan Metacraton, most notability in the form of migmatization and emplacement of high-K calc-alkaline granitoids (Shang et al., 2010; Fezaa et al., 2010).

5.4.2. Convective removal

Thermal erosion of cratonic roots through convective removal might not result in complete SCLM detachment at the crust-mantle boundary. Hence, it is possible that the uppermost part of the SCLM has survived such convective removal (Platt and Vissers, 1989). This might be another mechanism to explain the upper mantle structure of the Saharan Metacraton where the S-wave velocity model suggested the presence of a typical cratonic SCLM to a depth of ~100 km. Convective removal of the Saharan Metacraton's root might have stopped when the lithospheric equilibrium thickness reached ~100 km. Morency et al. (2002) used numerical modeling to show that cratonic roots thicker than the lithospheric equilibrium thickness can trigger basal and sideway convective flow capable of progressively thermally eroding the cratonic root. Furthermore, Morency et al. (2002) have shown that, depending on the root width, it might take between 50 and 750 Ma to remove the cratonic root up to the ~100 km lithospheric equilibrium thickness. Neoproterozoic destabilization events within the Saharan Metacraton diagnostic of asthenospheric ascendance to shallower levels support the notion that convective removal might have occurred at that time. These include emplacement of high-K calc-alkaline granitoids resulting from crustal melting induced by asthenospheric upwelling and widespread extension (Eaton, 1982; Lum et al., 1989).

5.4.3. Phanerozoic thermal events

Late Neoproterozoic remobilization of the Saharan Metacraton due to one or more tectonic or thermal events might have influenced younger deformation and igneous activity in the region (Guiraud et al., 2005). Indeed, the African plate was affected by Phanerozoic rifting as well as Cenozoic volcanism. The latter was interpreted by Ebinger and Sleep (1998) to manifest a mantle plume and by Liégeois et al. (2005) to result from the Africa–Europe convergence that can help explain the anomalous upper mantle structure beneath the Saharan Metacraton. However, we conclude that the Cenozoic mantle plume might not be the primary source of destabilization of the Saharan Metacraton, especially within its southern part. This is because material associated with the supposed plume is localized under Afar and it appears to spread westward following latitude 9°N as modeled by Ebinger and Sleep (1998). This observation is in good agreement with our differential S-wave velocity images which show negative values that extends westward from Afar (Fig. 2). In addition, with the current seismic data resolution, the Hoggar Swell (Fig. 4B) appears to be the only place close (~1000 km to the west) to the Saharan Metacraton where S-wave velocity anomalies suggestive of the presence of a hot spot are observed (Deen et al., 2006). This swell is considered to be associated with the Cenozoic mantle plume (Ebinger and Sleep, 1998). However, Liégeois et al. (2005) detailed a series of arguments against considering a mantle plume to be the source of the Hoggar Swell. Alternatively, Liégeois et al. (2005) favored a Cenozoic convergence between Africa and Europe, inducing reactivations of Neoproterozoic shear zones, to be the primary mechanism for the evolution of the swell. It remains to be seen from seismic data with better resolution whether or not other uplifted regions in North Africa with young volcanisms have seismic structures suggestive of the presence of mantle plume similar to that of the Hogar Swell.

6. Conclusions and recommendation for future research

The Saharan Metacraton shows an upper mantle structure that can be explained by partial loss of its cratonic root, and a SCLM typical of cratons that persists to at least a depth of 100 km. Such mantle structure might be due to mantle delamination or convective removal during the Neoproterozoic allowing for widespread emplacement of high-K calc-alkaline granitoids and migmatization at ~600 Ma. The Phanerozoic events were strongly influenced by the structure of the Saharan Metacraton, such as the Mesozoic rifts that encircle it and mark its boundaries. Much more geological, geochemical, geochronological, isotopic and geophysical studies are needed to fully understand the Saharan Metacraton.

Metacratonization and decratonization of cratons are subjects of great interest in the geosciences and the Saharan Metacraton might provide the scientific community (together with the North China Craton and the Wyoming Craton) the opportunity to examine the processes leading to the rise and demise of cratons. However, the Saharan Metacraton is one of the largest continental blocks on Earth that remains poorly understood. Hence, the metacraton is an ideal site for a multi-national scientific efforts. The recent detailed study of Fezaa et al. (2010) in the western part of the Saharan Metacraton is a good example of how the acquisition of new geological, geochronological and isotopic data can bring new constraints on these processes. We hope the present contribution will stimulate efforts to secure research funding from governmental agencies and petroleum and mining industries to undertake a systematic campaign to: (1) Collect geochemical, geochronological and isotopic data to better constraint the geological history of the metacraton, define its geochronological provinces, and understand its behavior as a geochemical-isotopic reservoir. (2) Deploy a reasonably-dense broadband seismic network to image the upper mantle structure of the metacraton and define its geophysical parameters. Most of the S-wave data used in this study and other studies (Begg et al., 2009) of the Saharan Metacraton were acquired through multi-bounce shear phases or surface waves. Deployment of broadband seismic network over the Saharan Metacraton will allow acquiring additional velocity data, hence improving the resolution of imaging the metacraton's upper mantle seismic structure. And (3) Conduct systematic mantle xenoliths studies to further constrain the upper mantle structure of the metacraton.

Acknowledgements

The idea of the Saharan Metacraton came from a series of discussions during the 18th Colloquium of African Geology, which was held in Graz, Austria in July 2000, hosted by the University

of Graz. We thank everyone who has contributed to this discussion. We thank Steve Grant for providing the seismic tomography data used in this study. We thank T. Kusky and R. Stern for constructive review. This is Missouri University of Science and Technology Geology and Geophysics Program contribution number 26.

References

Abdelsalam, M.G., Dawoud, A.S., 1991. The Kabus ophiolitic melange, Sudan, and its bearing on the western boundary of the Nubian Shield. Geological Society of London Special Publication 148, 83–92.

Abdelsalam, M.G., Stern, R.J., 1996. Mapping precambrian structures in the Sahara Desert with SIR-C/X-SAR radar: the Neoproterozoic Keraf Suture, NE Sudan. Journal of Geophysical Research 101 (E10), 23063–23076.

Abdelsalam, M.G., Liegeois, J.-P., Stern, R.J., 2002. The Saharan Metacraton. Journal of African Earth Sciences 34, 119–136.

An, M., Feng, M., Zhao, Y., 2009. Destruction of lithosphere within the North China Craton inferred from surface wave tomography. Geochemistry, Geophysics and Geosystems 10. doi:10.1029/2009GC002562.

Arndt, N.T., Coltice, N., Helmstaedt, H., Gregoire, M., 2009. Origin of Archean subcontinental lithopsheric mantle: some petrological constraints. Lithos 109, 61–71.

Artemieva, I.M., 2006. Global 1°X1° thermal model TC1 for the continental lithosphere: implication for lithosphere secular evolution. Tectonophysics 416, 245–277.

Artemieva, I.M., 2009. The continental lithosphere: reconciling thermal, seismic, and petrographic data. Lithos 109, 23–46.

Ashwal, L.D., Burke, K., 1989. African lithospheric structure, volcanism and topography. Earth Planetary Science Letters 96, 8–14.

Avigad, D., Gvirtzman, Z., 2009. Late Neoproterozoic rise and fall of the northern Arabian-Nubian Shield: the role of lithospheric mantle delamination and subsequent thermal subsidence. Tectonophysics 77, 217–228.

Begg, G.C., Griffin, W.L., Natapov, L.M., O'Reilly, S.Y., Grand, S., O'Neill, C.J., Hronsky, J.M.A., Poudjom Djomani, Y., Swain, C.J., Deen, T., Bowden, P., 2009. The lithospheric architecture of Africa: seismic tomography, mantle petrology, and tectonic evolution. Geosphere 5, 23–50.

Bendaoud, A., Ouzegane, K., Godard, G., Liégeois, J.P., Kienast, J.R., Bruguier, O., Drareni, A., 2008. Geochronology and metamorphic P–T–X evolution of the Eburnean granulite-facies metapelites of Tidjenouine (Central Hoggar, Algeria): witness of the LATEA metacratonic evolution. In: Ennih, N., Liégeois, J.-P. (Eds.), The Boundaries of the West African Craton, vol. 297. Geological Society of London Special Publication, pp. 111–146.

Bertrand, J.-M., Caby, R., 1978. Geodynamic evolution of the Pan-African orogenic belt: a new interpretation of the Hoggar Shield (Algerian Sahara). Geologische Rundschau 67, 357–388.

Bird, P., 1979. Continental delamination and the Colorado Plateau. Journal of Geophysical Research 84, 7561–7571.

Black, R., Liégeois, J.-P., 1993. Cratons, mobile belts, alkaline rocks and continental lithospheric mantle: the Pan-African testimony. Journal of the Geological Society, London 150, 89–98.

Burdick, S., van der Hilts, R.D., Vernon, F.L., Martynov, V., Cox, T., Eakins, J., Karasu, G.H., Tylell, J., Astiz, L., Pavlis, G.L., 2010. Model update January 2010: upper mantle heterogeneity beneath North America from traveltime tomography with global and USArray transportable array data. Seismological Research Letters 81, 689–693.

Davidson, J.P., Wilson, I.R., 1989. Evolution of an alkali basalt-trachyte suite from Jebel Marra Volcano, Sudan, through assimilation and fractional crystallization. Earth and Planetary Science Letters 95, 141–160.

De Waele, B., Liégeois, J.P., Nemchin, A.A., Tembo, F., 2006. Isotopic and geochemical evidence of Proterozoic episodic crustal reworking within the Irumide belt of South-Central Africa, the southern metacratonic boundary of an Archaean Bangweulu craton. Precambrian Research 148, 225–256.

Deen, T.J., Griffin, W.L., Begg, G., O'Reilly, S.Y., Natapov, L.M., Hronsky, J., 2006. Thermal and compositional structure of the subcontinental lithosphere mantle: derivation from shear wave seismic tomography. Geochemistry, Geophysics, Geosystems 7. doi:10.1029/2005GC001120.

Dugda, M.T., Nyblade, A.A., Julia, J., 2009. S-Wave velocity structure of the crust and upper mantle beneath Kenya in comparison to Tanzania and Ethiopia: implication for the formation of the East African and Ethiopian Plateaus. South African Journal of Geology 112, 241–250.

Dziewonski, A.M., Anderson, D.L., 1981. Preliminary reference Earth model. Physics of the Earth and Planetary Interiors 25, 297–356.

Eaton, G.P., 1982. The basin and range province:origin and tectonic significance. Annual Review of Earth Planetary Science 10, 409–440.

Eaton, D.W., Darbyshire, F., Evans, R.L., Grutter, H., Jones, A.G., Yuan, X., 2009. The elusive lithosphere – asthenosphere boundary (LAB) beneath cratons. Lithos 109, 1–22.

Ebinger, C.J., Sleep, N.H., 1998. Cenozoic magmatism throughout east Africa resulting from impact of a single plume. Nature 395, 788–791.

England, P., 1993. Convective removal of thermal boundary layer of thickened continental lithosphere; a brief summary of causes and consequences with special reference to the Cenozoic tectonics of the Tibetan Plateau and surrounding regions. Tectonophysics 223, 67–73.

Ennih, N., Liégeois, J.P., 2008. The boundaries of the West African craton, with a special reference to the basement of the Moroccan metacratonic Anti-Atlas belt. In: Ennih, N., Liégeois, J.-P. (Eds.), The Boundaries of the West African Craton, vol. 297. Geological Society of London Special Publication, pp. 1–17.

Fezaa, N., Liégeois, J.P., Abdallah, N., Cherfouh, E.H., De Waele, B., Bruguier, O., Ouabadi, A., 2010. Late Ediacaran geological evolution (575–555 Ma) of the Djanet Terrane, Eastern Hoggar, Algeria, evidence for a Murzukian intracontinental episode. Precambrian Research 180, 299–327.

Foster, D.A., Russo, R.M., Mueller, P.A., 2008. Delamination of the subcontinental lithosphere of the Wyoming Craton related to the Yellowstone Hot Spot. Geological Society of America Annual Meeting, Houston, TX 40, 329.

Grand, S.P., 2002. Mantle shear-wave tomography and the fate of subducted slabs. Philosophical Transactions – Royal Society. Mathematical, Physical and Engineering Sciences 360, 2475–2491.

Grand, S.P., Helmberger, D.V., 1984. Upper mantle shear structure of North America. Geophysical Journal International 76, 399–438.

Guiraud, R., Bosworth, W., Thierry, J., Delplanque, A., 2005. Phanerozoic geological evolution of Northern and Central Africa: an overview. Journal of African Earth Sciences 43, 83–143.

Henry, B., Liégeois, J.P., Nouar, O., Derder, M.E.M., Bayou, B., Bruguier, O., Ouabadi, A., Belhai, D., Amenna, M., Hemmi, A., Ayache, M., 2009. Repeated granitoid intrusions during the Neoproterozoic along the western boundary of the Saharan metacraton, Eastern Hoggar, Tuareg shield, Algeria: an AMS and U–Pb zircon age study. Tectonophysics 474, 417–434.

Hirth, G., Evans, R.L., Chave, A.D., 2000. Comparison of continental and oceanic mantle electrical conductivity. Is the Archean lithosphere dry? Geochemistry, Geophysics, Geosystems, 1, doi: 10.1029/2000GC000048.

Huang, J.L., Zhao, D.P., 2004. Crustal heterogeneity and seismotectonics of the region around Beijing, China. Tectonophysics 385, 159–180.

James, D.E., Fouch, M.J., VanDecar, J.C., van der Lee, S., 2001. Tectospheric structure beneath southern Africa. Geophysical Research Letters 28, 2485–2488.

Kay, R.W., Kay, S.M., 1993. Delamination and delamination magmatism. Tectonophysics 219, 177–189.

Keller, G.R., 2008. Is the Woyoming Craton being decratonized? Geological Society of America Annual Meeting, Houston, TX 40, 329–330.

Kennedy, W.Q., 1964. The structural differentiation of Africa in the Pan-African (500 Ma) tectonic episode: Annual Report of the Research Institute of African Geology. University of Leeds 8, 48–49.

King, S.D., Ritsema, J., 2000. African hot spot volcanisms: small-scale convection in the upper mantle beneath cratons. Science 29, 1137–1140.

Klerkx, J., Deutsch, S., 1977. Resultats preliminaires obtenus par la methode Rb/Sr sur l'age des formations precambriennes de la region d'Uweinat (Libye): Musee Royal de l'Afrique Centrale. Département Géologie Minéralogie Rapport Annuel 83, 94.

Kröner, A., 1977. The Precambrian geotectonic evolution of Africa: plate accretion vs. plate destruction. Precambrian Research 4, 163–213.

Kusky, T.M., Windley, B.F., Zhai, M.G., 2007a. Lithospheric thinning in eastern Asia; constraints, evolution, and tests of models. In: Zhai, M.G., Windley, B.F., Kusky, T.M., Meng, Q.R. (Eds.), Mesozoic Sub-Continental Lithospheric Thinning Under Eastern Asia, vol. 280. Geological Society of London Special Publication, pp. 331–343.

Kusky, T.M., Windley, B.F., Zhai, M.G., 2007b. Tectonic evolution of the North China block: from Orogen to Craton to Orogen. In: Zhai, M.G., Windley, B.F., Kusky, T.M., Meng, Q.R. (Eds.), Mesozoic Sub-Continental Lithospheric Thinning Under Eastern Asia, vol. 280. Geological Society of London Special Publication, pp. 1–34.

Küster, D., Liégeois, J.P., Matukov, D., Sergeev, S., Lucassen, F., 2008. Zircon geochronology and Sr, Nd, Pb isotope geochemistry of granitoids from Bayuda Desert and Sabaloka (Sudan): evidence for a Bayudian event (920–900 Ma) preceding the Pan-African orogenic cycle (860–590 Ma) at the eastern boundary of the Saharan Metacraton. Precambrian Research 164, 16–39.

Lebedev, S., Boonen, J., Trampert, J., 2009. Sesmic structure of Precambrian lithosphere: new constraints from broad-band surface wave dispersion. Lithos 109, 96–111.

Liégeois, J.P., Black, R., Navez, J., Latouche, L., 1994. Early and late Pan-African orogenies in the Aïr assembly of terranes (Tuareg Shield, Niger). Precambrian Research 67, 59–88.

Liégeois, J.P., Latouche, L., Boughrara, M., Navez, J., Guiraud, M., 2003. The LATEA metacraton (Central Hoggar, Tuareg shield, Algeria): behaviour of an old passive margin during the Pan-African orogeny. Journal of African Earth Sciences 37, 161–190.

Liégeois, J.P., Benhallou, A., Azzouni-Sekkal, A., Yahiaoui, R., Bonin, B., 2005. The Hoggar swell and volcanism: reactivation of the Precambrian Tuareg shield during Alpine convergence and West African Cenozoic volcanism. In: Foulger, G.R., Natland, J.H., Presnall, D.C., Anderson, D.L. (Eds.), Plates Plumes and Paradigmsm, vol. 388. Geological Society of America Special Paper, pp. 379–400.

Lucassen, F., Franz, G., Romer, R.L., Bulski, P., 2008. Late Cenozoic xenoliths as a guide to the chemical-isotopic composition and thermal state of the upper mantle under northern Africa. European Journal of Mineralogy 20, 1079–1096.

Lum, C.C.L., Leeman, W.P., Foland, K.A., Kargell, J.A., Fitton, J.G., 1989. Isotopic variation in continental basaltic lavas as indicators of mantle heterogeneity: examples from the western US Cordillera. Journal Geophysical Research 94, 871–884.

Meert, J.G., Lieberman, B.S., 2007. The Neoproterozoic assembly of Gondwana and its relationship to the Ediacaran-Cambrian radiation. Gondwana Research. doi: 10.1016/j.gr.2007.06.007.

Morency, C., Doin, P.M., Dumoulin, C., 2002. Convective destabilization of a thickened continental lithosphere. Earth and Planetary Science Letters 202, 303–320.

O'Reilly, S.Y., Griffin, W.L., Poudjom Djomani, Y.H., Morgan, P., 2001. Are lithospheres forever? Tracking changes in subcontinental lithospheric mantle through time. GSA Today 11, 4–10.

Pasyanos, M.E., 2010. Lithospheric thickness modeled from long-period surface wave dispersion. Tectonophysics 481, 38–50.

Pasyanos, M.E., Nyblade, A.A., 2007. A top to bottom lithopsheeric study of Africa and Arabia. Tectonophysics 444, 27–44.

Pin, C., Poidevin, J.L., 1987. U–Pb zircon evidence for a Pan-African granulite facies metamorphism in the Central African Republic. A new interpretation of the high-grade series of the northern border of the Congo Craton. Precambrian Research 36, 303–312.

Platt, J.P., Vissers, R.L.M., 1989. Extensional collapse of thickened continental lithosphere: a working hypothesis for the Alboran Sea and Gibraltar Arc. Geology 17, 540–543.

Pollack, H.N., 1986. Cratonization and thermal evolution of the mantle. Earth and Planetary Science Letters 80, 175–182.

Priestley, K., McKenzie, D., Debayle, E., 2006. The state of the upper mantle beneath Southern Africa. Tectonophysics 416, 101–112.

Ritsema, J., van Heijst, H., 2000. New seismic model of the upper mantle beneath Africa. Geology 28, 63–66.

Rocci, G., 1965. Essai d'interpretation de mesures geochronologiques. La structure de l'Ouest africain. Sciences Terre Nancy 10, 461–479.

Santosh, M., Zhao, D., Kusky, T., 2010. Mantle dynamics of the Paleoproterozoic North China Craton: a perspective based on seismic tomography. Journal of Geodynamics 49, 39–53.

Schott, B., Schmeling, H., 1998. Delamination and detachment of a lithospheric root. Tectonophysics 296, 225–247.

Shang, C.K., Satir, M., Morteani, G., Taubald, H., 2010. Zircon and titanite age evidence for coeval granitization and migmatization of the early Middle and early Late Proterozoic Saharan Metacraton; example from the central North Sudan basement. Journal of African Earth Sciences. doi: 10.1016/j.jafrearsci.2009.12.006.

Shapiro, N.M., Ritzwoller, M.N., 2002. Monte-Carlo inversion for a global shear-velocity model of the crust and upper mantle. Geophysical Journal International 151, 88–105.

Stern, R.J., 1994. Arc assembly and continental collision in the Neoproterozoic E African Orogen: implication for the consolidation of Gondwanaland. Annual Review of Earth Planetary Science 22, 319–351.

Stern, R.J., Kröner, A., Reischmann, T., Bender, R., Dawoud, A.S., 1994. Precambrian basement around Wadi Halfa: a new perspective on the evolution of the Central Saharan Ghost craton. Geologische Rundschau 83, 564–577.

Sultan, M., Tucker, R.D., El Alfy, Z., Attia, R., Ragab, A.G., 1994. U–Pb (zircon) ages for the gneissic terrane west of the Nile, southern Egypt. Geologische Rundschau 83, 514–522.

Tian, Y., Zhao, D., Sun, R., Teng, J., 2009. Seismic imaging of the crust and upper mantle beneath the North China Craton. Physics of the Earth and Planetary Interiors 172, 169–182.

Toteu, S.F., Fouateu, R.Y., Penaye, J., Tchakounte, J., Seme Mouange, A.C., Van Schmus, W.R., Deloule, E., Stendal, H., 2006. U–Pb dating of plutonic rocks involved in the nappe tectonic in southern Cameroon: consequence for the Pan-African evolution of the central African fold belt. Journal African Earth Sciences 44, 479–493.

van der Lee, S., Nolet, G., 1997. Upper mantle S velocity structure of North America. Journal of Geophysical Research 102, 22815–22838.

Yang, J.-H., Wu, F.-Y., Wilde, S.A., Belousova, E., Griffin, W.L., 2008. Meoszoic decratonization of the North China block. Geology 36, 467–470.

Zhai, M.G., Windley, B.F., Kusky, T.M., Meng, Q.R., 2007. Mesozoic sub-continental lithospheric thinning Under Eastern Asia. Geological Society of London Special Publication 280, 352, ISBN:978-1-86239-225-0.

Zhao, L., Allen, R.M., Zheng, T., Hung, S.H., 2009. Reactivation of an Archean craton: constaints from P- and S-wave tomography in North China. Geophysical Research letters 36. doi:10.1029/2009GL039781.